IRAQI Academic Scientific Journals
Samarra Journal of Pure and Applied Science
SJPAS
www.sjpas.com
p ISSN: 2663-7405
e ISSN: 2789-6838

Effect of Doping with Zinc Oxide on The Structural, Surface, and Optical Properties of Titanium Dioxide Thin Films

Hayim Ch Magid[1], Hiba Saad Rasheed[1], Rusul Adnan Al-Wardy[2*]
1- Department of physics, College of Education, Mustansiriyah University, Baghdad, Iraq.
2- Department of clinical Laboratory science, College of pharmacy, Mustansiriyah University, Baghdad, Iraq.

https://doi.org/10.54153/sjpas.2023.v5i2.500

Article Information
Received: 19/03/2023
Accepted: 26/04/2023

Keywords:
Titanium Dioxide, Zinc doping, Spray pyrolysis technique, XRD, AFM.

Corresponding Author
E-mail:
dr.rusuladnan@uomustansiriyah.edu.iq

Abstract

Titanium oxide thin films that are both undoped and doped with zinc have been produced in rates of (0, 2 and 4) %. The titanium oxide films doped with zinc are made by combining cadmium acetate with zinc acetate in a solution of titanium acetate with (0.2 M). X-ray diffraction tests show that the films of undoped TiO_2 and (TiO_2: Zn) are polycrystalline with (121) orientation. Additionally, the crystallization of films rises as zinc doping level rises. With zinc doping concentration, the grain size of the deposited films is around (15.55-17.91) nm, while the strain (%) parameter decreases from 22.29 to 19.35 with zinc. The grain size is in the range of (90.9), (67.8), and (37.7) nm for the (Ti O_2, TiO_2: 2% Zn, and TiO_2:4% Zn) accordingly in Atomic Force Macroscopy pictures of the film surface morphology. Surface roughness and rms values for the deposited films for undoped TiO_2 and TiO_2:2% Zn, and TiO_2:4%Zn are (6.72, 3.34, and 2.034) nm and (8.80, 8.03, and 4.24), respectively. The spectrum of absorbance and transmission is used to study the optical characteristics. The investigation revealed that the films have robust transmission throughout the visible spectrum and that this transmission decreases with increased doping with zinc content. In addition, the edge of the films' absorbance changes to high wavelengths, which supports a drop in energy gap values. Also computed and discovered to vary with increased doping with zinc concentration are the absorption coefficient, refractive index, and extinction coefficient.

Introduction

Titanium dioxide (TiO_2) semiconductor has been subjected to the greatest amount of research because it possesses many very desirable physical characteristics. These characteristics include long-term stability, oxidative ability, broad band gap, low cost, and minimal biological toxicity [1]. TiO_2 has the outstanding proportion of excellent transmittance in visible and high refractive index, as well as chemical stability and as high electrical [2]. It is extensively employed in many applications, like photocatalysts [3, 4], supercapacitors [5,6], LED [6,7], and biosensors [8]. Numerous studies have recently focused on the doping of titanium dioxide with transition metals (such as Fe [9], Co [10], Mn [11,12], and Ni [13]. According to literature, Mn is one of ideal ions for doping TiO_2 because it may increase the photocatalytic efficiency [11]. TiO_2 thin films were produced using a variety of synthetic

methods, including thermal [14,15], the sol-gel technique [16,17], plasma spray [18], PLD [19,20], RF sputtering method [21,22], and the Spray Pyrolysis Technique [1,5,11, 23–26]. Among these, the spray pyrolysis process offers many benefits, including ease of use, homogeneity, repeatability, and permits to prepare cover layers with large areas and easily apply for industrial manufacture, and the ability to add dopants with regulated atomic content in the sprayed solution. This investigation's goal is to learn more about the impact.

Experimental

Using an integrated spray pyrolysis method unit, thin films of undoped TiO_2 and TiO_2: Zn were deposited; the right proportions of titanium chloride (0.2M) dissolved in deionized water were combined to create the spray solution. Zinc trichloride (Zn Cl_3) was dissolved in isopropyl alcohol and added to the precursor solution to obtain zinc doping. The spray solution comprised 60 ml and had a doping concentration of (0, 2, 4) %. The requirements for preparation: The substrate was heated to 450 °C, the spout was 31 cm away from the base, the spraying duration was extended by 90 seconds to prevent cooling, the spray rate was 6 mL/min, and N_2 was utilized as the carrier gas. The film's thickness was determined to be 325 ± 20 nm using the weighing method, equation (1).

The following relation used to get the weight of solution within the above molarity:

$$M = \left(\frac{W_t}{M_{wt}}\right).\left(\frac{1000}{V}\right) \qquad (1)$$

M: concentration molarity.
W_t: weight of solution.
V: volume of water.
M_{wt}: molecular weight of titanium chloride.
It has been found that the following deposition parameters give good films with good transparency and uniform surface.
Film structure was ascertained using XRD, and the surface of the thin films that had been deposited was examined using AFM. Using a UV-visible shimadzu double-beam spectrophotometer to obtain transmittance spectra.

Result and Discussion

Figure 1 shows the XRD pattern of the grown films. It presents two firm peaks that, respectively, correlate to the anatase (111), (121), (022), (241) and (203) planes at 2 = 25.61°, 30.78°, 40.15°, 55.73°, and 64.12°. A peak of 121 was observed, matching ICDD card numbers 29-1360 [5].

The reason for the absence of peaks related to magnesium in the X-ray diffraction (XRD) pattern is that there are only a small number of metal ion dopants and the zinc ions are dispersed within the titanium dioxide lattice [27]. As the concentration of zinc is increased, the peak density in the XRD pattern of the zinc -doped titanium dioxide poly-scales becomes higher, leading to the formation of more stable and well-crystalline phases, In other words, the presence of zinc helps to enhance the crystal structure of magnesium-doped titanium dioxide and improves its stability [28].

The grain size D was obtained from Scherrer's equation [29]:

$$D = \frac{0.9\lambda}{\beta cos\theta} \qquad (2)$$

Where β is the full-width half maximum (FWHM) of the diffraction peak, θ is the diffraction angle, and λ is the X-ray wavelength. The information collected is presented in Table 1, which shows that an increase in the zinc concentration results in an increase in the grain size from 15.55 to 17.91 nm. This indicates that the concentration of zinc plays a crucial role in determining the diameter of material crystals. As the concentration of zinc increases, it causes a larger crystal structure to form, which in turn leads to an increase in the grain size of the material [30].

To calculate the dislocation density (δ) in thin films, the following equation (3) is used[29]:

$$\delta = \frac{1}{D^2} \qquad (3)$$

Table 1 presents the data indicating that the dislocation density decreased from 41.35 to 31.17 as the zinc doping content increased. This suggests that the addition of zinc can help to reduce the number of dislocations in the material, leading to an improvement in its structural quality [31].

The strain (ε) was estimated using the following equation [27]:

$$\varepsilon = \frac{\beta cos\theta}{4} \qquad (4)$$

The information presented in Table 1 demonstrates that an increase in zinc doping level causes the strain parameter's value to decrease from 22.29 to 19.35. This indicates that the presence of zinc can help to improve the structural quality of the material by reducing its internal strain. The table also shows the resulting structural coefficients for each doping level [32].

FWHM and D are shown in Fig. 2 as being against a zinc doping concentration. The figure displayed the structural S_{para} values as shown in Table 1.

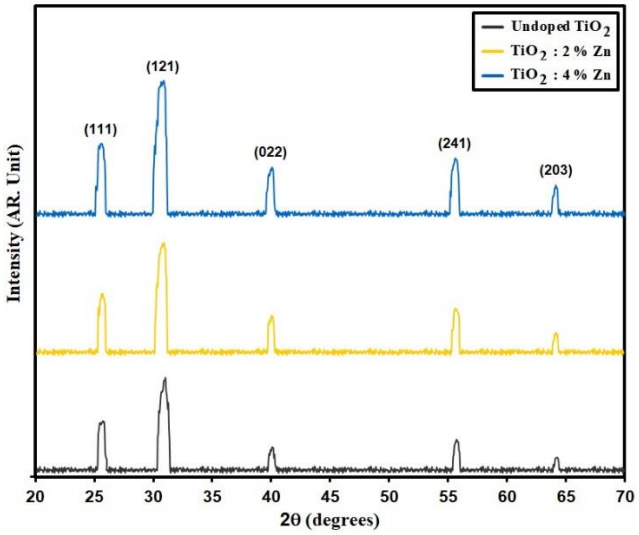

Fig. 1 XRD-patterns Variation for undoped and Zn doped TiO_2 thin films.

Table 1: The grain size *D*, energy gap E_g and S_{para} for undoped and Zn doped TiO_2 thin films.

Samples	2 θ (°)	(hkl) Plane	FWHM (°)	E_g (eV)	*D* (nm)	δ (×10^{14})(lines/m^2)	ε×10^{-4}
Undoped TiO_2	30.78	121	0.53	3.24	15.55	41.35	22.29
TiO_2: 2% Zn	30.74	121	0.50	3.19	16.48	36.82	21.03
TiO_2: 4% Znr	30.69	121	0.46	3.13	17.91	31.17	19.35

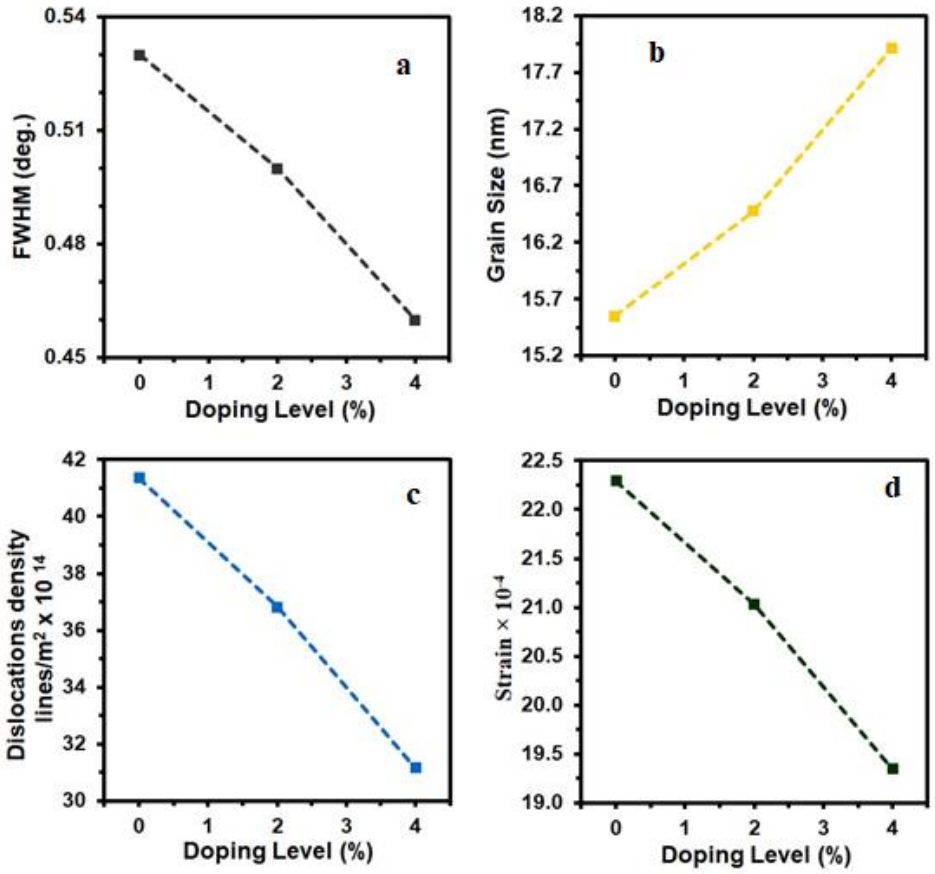

Fig. 2 S_{para} of intended films. a) FWHM, b) grain size, C) dislocation density lines, D) strain versus doping level for undoped TiO_2 and Zn doped TiO_2 thin films.

The AFM micrograph for thin films of TiO_2 and TiO_2: Zn is shown in Fig. 3. Undoped TiO_2 and TiO_2: Zn films had average particle sizes and surface roughness values of 90.9, 67.8 and 37.7 nm and 6.72, 3.26 and 2.344 nm for TiO_2, TiO_2: 2% Zn, and TiO_2: 4% Zn, respectively. By raising TiO_2 and TiO2: 4% Zn, the RMS was reduced from 8.80 nm to 4.24 nm. The Atomic Force Microscopy (AFM) results demonstrate that the average particle size and roughness of the film decrease with an increase in zinc concentration. This suggests that the film's crystallinity has improved and there is a reduction in defects. These values provide evidence that the film is in a nanocrystalline state [33]. Table 2 lists the values of AFM parameters P_{AFM}.

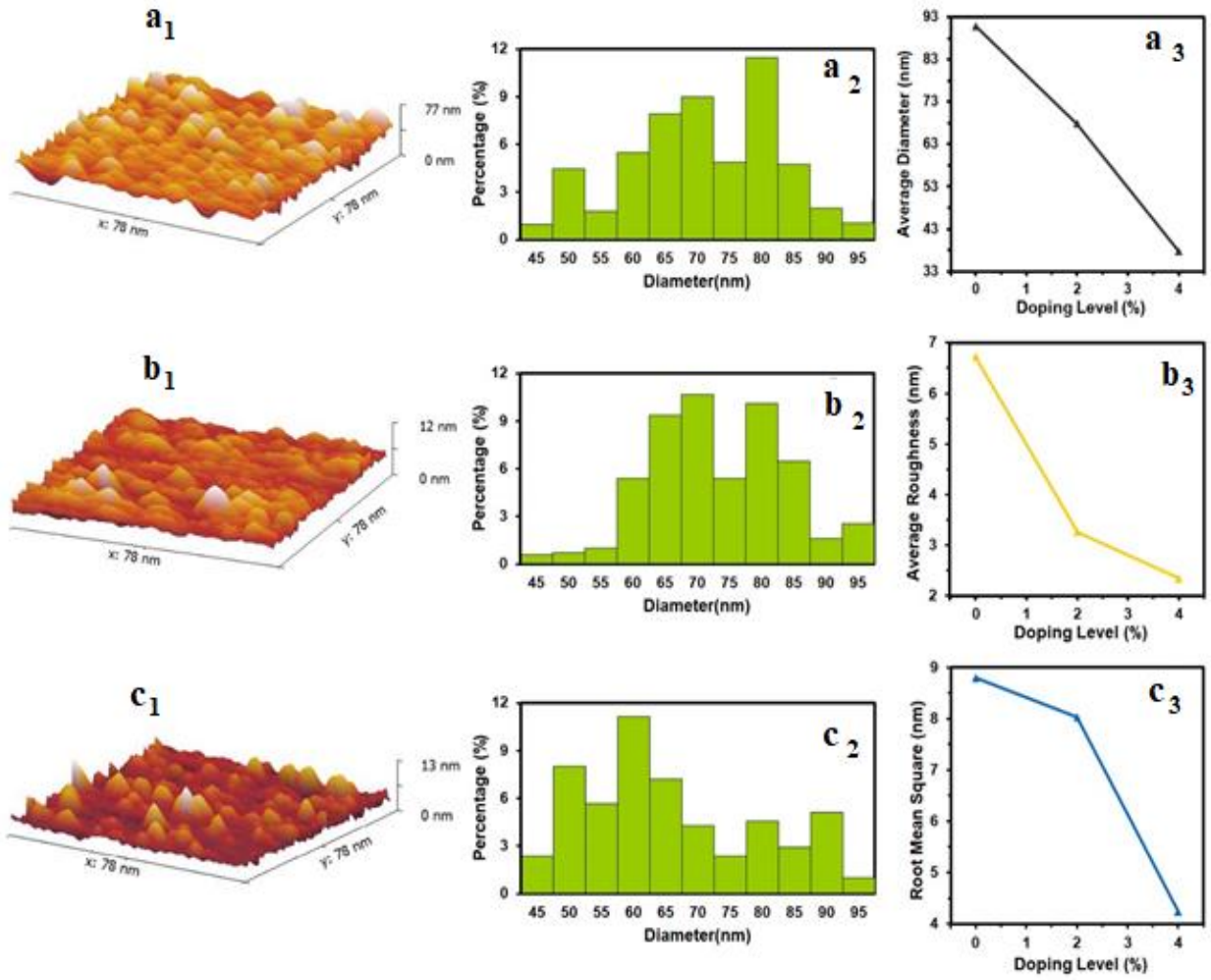

Fig. 3 AFM information, average particle sizes and surface roughness for a) undoped b) 2% doped c) 4% Zn doped TiO_2 thin films.

Table 2: P_{AFM} for undoped and Zn doped TiO_2 thin films.

Samples	Average Particle size nm	average surface roughness (nm)	rms (nm)
Undoped TiO_2	90.9	6.72	8.80
TiO_2: 2% Zn	67.8	3.26	8.03
TiO_2: 4% Zn	37.7	2.34	4.24

Figure. 4 offers the transmittance (T) spectra of TiO_2 and TiO_2: Zn. With increasing zinc doping levels, transmittance in the UV-Vis region declined until it reached over 86% transmittance at undoped TiO_2 thin films, these results are consistent with other published results such as results [24,25].

The absorption coefficient α can be evaluated by the formula [34]:

$$(2.303 \times A)/t = \alpha \qquad (5)$$

Where the film thickness is (t), the absorption coefficient for undoped TiO_2 and TiO_2 is shown in Figure 5. The impact of the zinc doping concentration was linked to the discovery that Zn thin films give absorption coefficient increases with increasing Zn and with rising with the relation that may be used to determine the energy gap (Eg) [35]:

$$(\alpha h\nu) = A\left(h\nu - E_g\right)^{\frac{1}{2}} \qquad (6)$$

Where A is absorbance and $h\nu$ is photon energy. Plots of incident photon energy $(\alpha h\nu)^2$ against $(h\nu)$ were produced. The diagrams are shown in Figure 6. Energy gap dropped from 3.24 to 3.13 eV with 4% Cr doping level because TiO_2 and TiO_2: Zn films are direct transition semiconductors [26]. difference of the band gap energies is depending on the degree of crystallinity and different doping concentration [11].

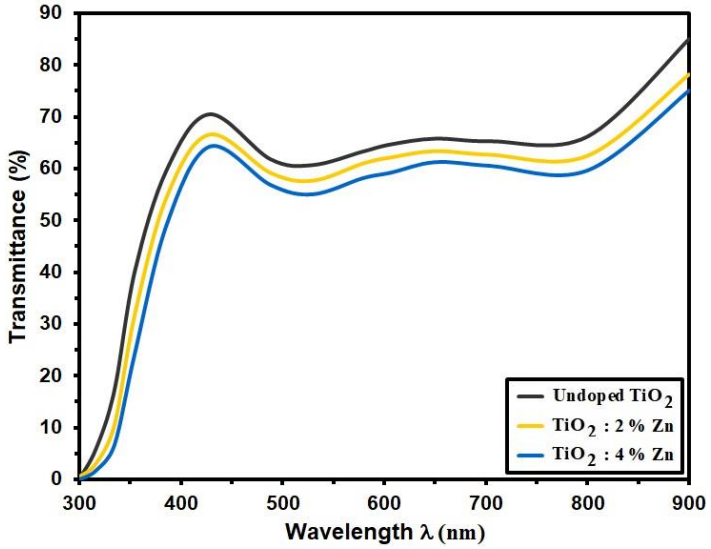

Fig. 4 The transmittance versus wavelength (λ) for undoped and Zn doped TiO_2 thin films.the grown films.

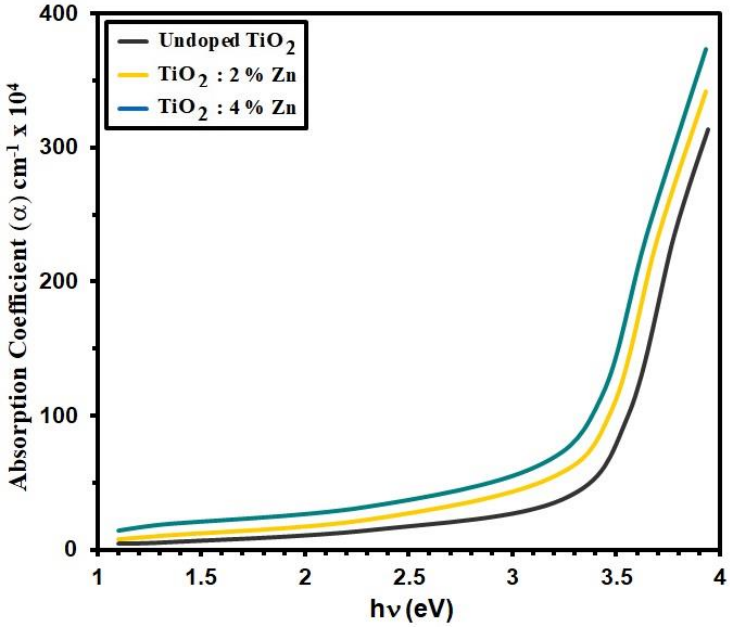

Fig. 5 Absorption coefficient for undoped and Zn doped TiO_2 thin films.of grown films.

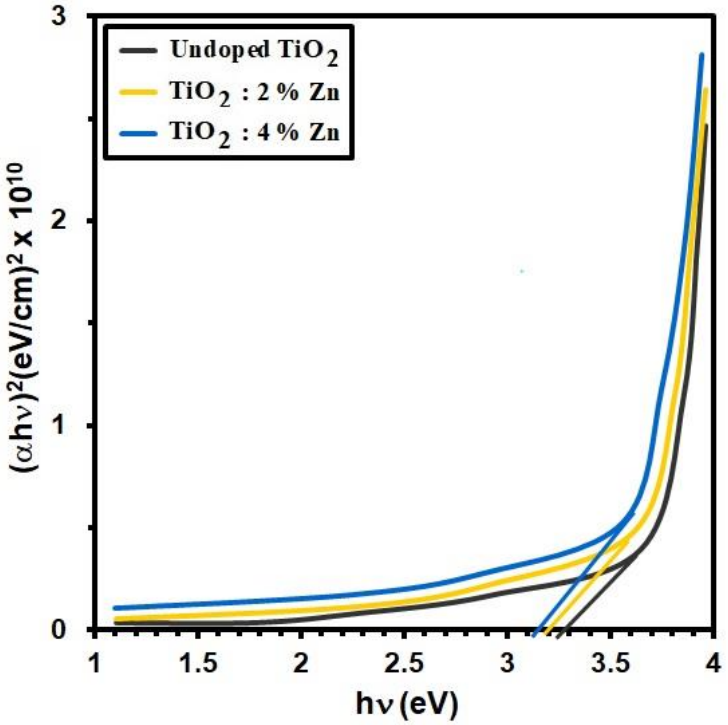

Fig. 6 Energy gap for undoped and Zn doped TiO_2 thin films.

The extinction coefficient (k) can be estimated from the relation [36]:

$$k = \frac{\alpha\lambda}{4\pi} \qquad (7)$$

The relationship between extinction coefficient and wavelength are plotted in Fig.7 for zinc-doped TiO_2 thin film. It can notice that the extinction coefficient decreased with increasing zinc doping content and wavelength. It can be seen that the lowest value of (k) for TiO_2 films by using TiO_2: 4% Zn concentration that indicates to lowest surface roughness [31].

The refractive index (n) relayed on reflectance R and *k* by the relation[37]:

$$n = \left[\left(\frac{4R}{(R-1)^2}\right) - K_0^2\right]^{1/2} - \frac{R+1}{R-1} \qquad (8)$$

Fig.8 shows that n decreases with increasing zinc doping content. In addition, the decreased of Refractive index of undoped TiO_2 and (TiO_2: Zn) sprayed in the end of visible and near IR region is relating to increase of carrier concentration [38-40].

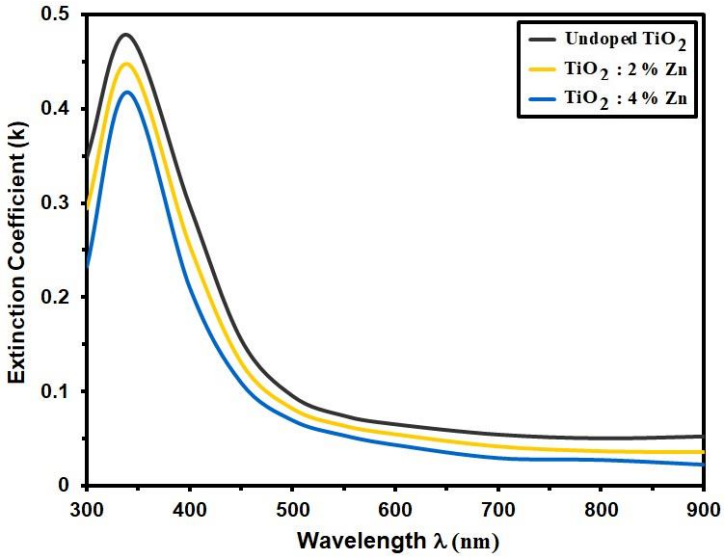

Fig. 7 Variation of Extinction coefficient (k) versus wavelength (λ) for undoped and Zn doped TiO_2 thin films.

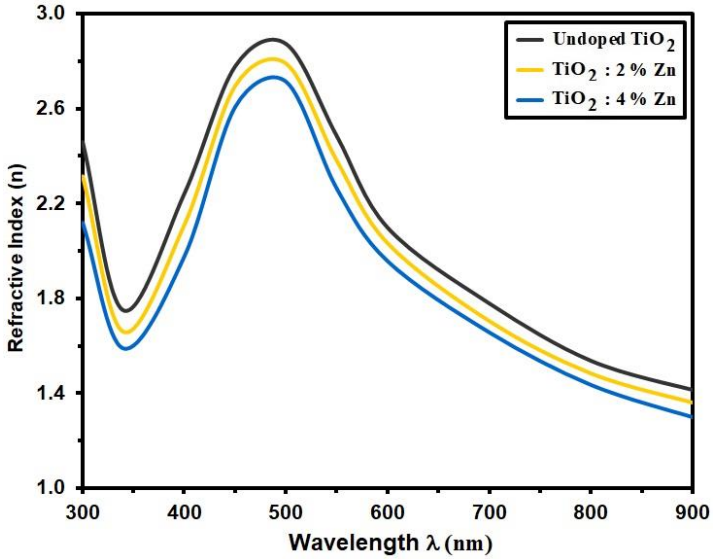

Fig. 8 Variation of Refractive index (n) versus wavelength (λ) for undoped and Zn doped TiO_2 thin films.

Conclusion

Chemical spray pyrolysis (CSP) was used to create films of undoped TiO_2 and TiO_2: 2% Zn. At 400 ^oC, these films are produced on glass substrates. When TiO_2 was doped, grain size increased from 15.55 nm to 17.91 nm, according to XRD, while dislocation density and strain decreased from (41.35 to 31.17), and the high peak matched the (121) plane (22.29 to 19.35). In Undoped TiO_2 thin films, the AFM picture revealed that average Particle Size rises from (90.9 to 37.7 nm), Surface Roughness and rms values decrease with increasing Zinc Doping Content. Transmittance spectra showed that the near-infrared region of titanium oxide had high values. The absorption coefficient increases as the amount of doped zinc do. As the amount of doped zinc increased, the values of Eg were in the range of 2.20–2.10 eV. As zinc doping level rises, so do the extinction coefficient and refractive indices.

References

1. Silva-Osuna, E.R.,Vilchis-Nestro, A.R.,Villarreal-Sanchez, R.C., Castro-Beltran, A. & Luque, P.A. (2022). Study of the optical properties of TiO2 semiconductor nanoparticles synthesized using Salvia rosmarinus and its effect on photocatalytic activity Optical materials, vol. 124, 112039,.https://doi.org/10.1016/j.optmat.2022.112039
2. Alsulami, Q. A.& Rajeh, A. (2022). Structural, thermal, optical characterizations of polyaniline/polymethyl methacrylate composite doped by titanium dioxide nanoparticles as an application in optoelectronic devices Optical materials, vol.123, 111820, https://doi.org/10.1016/j.optmat.2021.111820
3. Khan, M. I. (2021). Investigations the structural, optical and photovoltaic properties of La doped TiO2 photoanode based dye sensitized solar cells Optical materials, vol.122, part A, 111610,. https://doi.org/10.1016/j.optmat.2021.111610
4. Chenaina, H., Messaadi, C.& Jalali, J. (2021). Study of structural, optical and electrical properties of SnO2 doped TiO2 thin films prepared by a facile Sol-Gel route inorganic chemistry communications, vol.124, 108401, https://doi.org/10.1016/j.inoche.2020.108401
5. Mokrushin, A. S. (2019) Oxygen detection using nanostructured TiO2 thin films obtained by the molecular layering method Applied surface science, vol.463, , p. 197-202. https://doi.org/10.1016/j.apsusc.2018.08.208
6. Saleh,A. F., Jaffar, A. M., Samoom, N. A. & Mahmmod, M. W.(2014) Effect Adding PVA Polymer on Structural and Optical Properties of TiO2 Thin Films Journal of Al-Nahrain University Vol.17 (2), pp.116-121.
7. Zeribi,F., Attaf,A., Derbali,A., Saidi,H., Benmebrouk,L., Aida, M.S., Dahnoun,M., Nouadji, R. & Ezzaouia, H. (2022) Dependence of the Physical Properties of Titanium Dioxide (TiO2) Thin Films Grown by Sol-Gel (Spin-Coating) Process on Thickness ECS Journal of Solid State Science and Technology 11 023003. DOI 10.1149/2162-8777/ac5168
8. Abdullah, M. T., Dagher, H.F. & Abd, A. N.(2021) Study on the optical and structure properties of TiO2 for different thickness prepared by spray pyrolysis Journal of Physics: Conference Series 1999 012131 DOI 10.1088/1742-6596/1999/1/012131
9. Al-mashary, F.S., Felix, J.F., Ferreira, S. O. & Alyamani, A. Y. (2020) Investigation of the structural, optical and electrical properties of indium-doped TiO2 thin films grown by Pulsed Laser Deposition technique on low and high index GaAs planes Materials Science and Engineering: B Volume 259, 114578. https://doi.org/10.1016/j.mseb.2020.114578
10. Alghamdi, H.M. & Rajeh, A. (2021) Synthesis of carbon nanotubes/titanium dioxide and study of its effect on the optical, dielectric, and mechanical properties of polyvinyl alcohol/sodium alginate for energy storage devices international journal of energy research vol. 46, issue 14 https://doi.org/10.1002/er.7578
11. Kala, P. V. , Rao, B. T. & Srinivasarao, K. (2019) Structural, optical and gas sensing properties of TiO 2-MoO3 thin films international journal of thin films science and technology 8, no.3, 163-174.
12. Yang, L., Luo, X., Yang, F., Liu, C., Zhang, L. & Tang, J. (2020) Electronic structure and optical properties of C-Pt codoped anatase TiO2 by first principles Optik Volume 223, 165588. https://doi.org/10.1016/j.ijleo.2020.165588

13. Ehsan,M. A., Shah, S. S., Basha, S. I., Hakeem, A. S. & Abdul Aziz, Md. (2021) Recent Advances in Processing and Applications of Heterobimetallic Oxide Thin Films by Aerosol-Assisted Chemical Vapor Deposition the chemical record, a journal of the chemical society of Japan, vol.22, issue 7 https://doi.org/10.1002/tcr.202100278
14. Mols, K., Arik, L., Mandar, H., Kasikov, A., Niilisk, A., Rammula, R.& Arik, J. (2019) Influence of phase composition on optical properties of TiO2: Dependence of refractive index and band gap on formation of TiO2-II phase in thin films Optical Materials, vol. 96, 109335 https://doi.org/10.1016/j.optmat.2019.109335
15. Lee, J., Moon, S., Patil, S. S. & Lee, K. (2022) Visible photoresponse of TiO2 nanotubes in comparison to that of nanoparticles and anodic thin film catalysis today, vol.403, p. 39-46. https://doi.org/10.1016/j.cattod.2022.01.008
16. Lang, J., Takahashi, K., Kubo, M. & Shimada, M. (2022) Preparation of TiO2-CNT-Ag Ternary Composite Film with Enhanced Photocatalytic Activity via Plasma-Enhanced Chemical Vapor Deposition catalysts, 12(5), 508. https://doi.org/10.3390/catal12050508
17. Mazumder, J. T., Mayengbam, R., Nath, A. & Sarkar, M. B. (2022) Investigation of structural, optical and electrical properties of TiO2 thin film-nanowire-based device for photodetector application optical materials , vol. 133, 112936 https://doi.org/10.1016/j.optmat.2022.112936
18. Seema, Kumar, N. & Chand, S. (2023) Structural, morphological, optical and dielectric properties of Ti1-xFexO2 nanoparticles synthesized using sol-gel method Journal of Sol-Gel Science and Technology vol. 105, pages 163–175.
19. Sharma, A., Gouldstone, A., Sampath, S. & Gambino,R. J.(2006) Anisotropic electrical conduction from heterogeneous oxidation states in plasma sprayed TiO2 coatings J. Appl. Phys., Vol. 100, 114906
20. Abdullah, A.Z., Haider, A. J. & Jabbar, A. A. (2022) Preparation of TiO2 nano-thin films by pulsed laser deposition: A review AIP Conference Proceedings 2437, 020092 https://doi.org/10.1063/5.0093012
21. Daughtry,J., Alotabi, A.S., Howard-Fabretto, L.& Andersson, G. G. (2021) Composition and properties of RF-sputter deposited titanium dioxide thin films Nanoscale Adv., 3, 1077-1086 DOI: 10.1039/D0NA00861C
22. Fouda, A.N.(2020) Influence of deposition temperature on the structural and dispersion parameters of TiO2 thin films Applied Physics A, 126(48).
23. Wang, L., Yang, J., Zhao, H., Liu, Y., Han, G. & Wang, J. (2022) Structural, optical and electrical properties of r-TiO2:Sn/SnO2:(F/Nb) tandem film by aerosol-assisted chemical vapor deposition surfaces and interfaces, vol.33, 102196. https://doi.org/10.1016/j.surfin.2022.102196
24. Sivaranjan, V. , Deepa, P. & Philominathan,P.(2015) Thin Films of TiO2-MoO3 Binary Oxides Obtained by an Economically Viable and Simplified Spray Pyrolysis Technique for Gas Sensing Application International Journal of Thin films Science and Technology, No. 2, 125-131
25. Radic, N., Grbic, B., Petrovic, S., Stojadinovic, S., Tadic, N.& Stevanov, P. (2020) Effect of cerium oxide doping on the photocatalytic properties of rutile TiO2 films prepared by spray pyrolysis Physica B: condenced Matter, vol.599, 412544. https://doi.org/10.1016/j.physb.2020.412544
26. Oja, I., Mere, A., Krunks, M., Solterbeck, C-H.& Es-Sount, M. (2004) Properties of TiO2 Films Prepared by the Spray Pyrolysis Method solid state phenomena, 99-100, 259-264.

27. Zhang, M., Wang, Z., Song, X., & Wu, J.(2011) Enhanced photocatalytic activity of Zn-doped TiO2 nanoparticles prepared via a sol-gel method, Journal of Sol-Gel Science and Technology, vol. 60, no. 3, pp. 393-400.
28. Vijayalakshmi, K., Ramalingam,V., & Thirumal S.(2014) Influence of Zinc dopant on the structural and optical properties of TiO2 nanoparticles prepared by co-precipitation method, Journal of Alloys and Compounds, vol. 617, pp. 40-45.
29. Jafari, A. & Loghman-Estarki,M. R.(2022), Synthesis, characterization and photocatalytic activity of zinc-doped titanium dioxide nanoparticles, Journal of Physics and Chemistry of Solids, vol. 168, pp. 109528.
30. Ahmed, N. S. et al.(2021), Effect of Zinc Doping on the Structural and Optical Properties of TiO2 Thin Films, Materials Today: Proceedings, vol. 45, pp. 125-129.
31. Ghasemi, S., Rahimi-Nasrabadi, M.& Ghasemi, M. (2016), Synthesis and characterization of Zn-doped TiO2 nanoparticles via sol-gel method: Investigation of the effect of calcination temperature on photocatalytic activity, Journal of Sol-Gel Science and Technology, vol. 78, no. 3, pp. 575-586.
32. Kimm M. G., Lim, J. H., & Kang, Y. S.,(2022) Enhanced photocatalytic activity of Zn-doped TiO2 nanorods synthesized by hydrothermal method, Journal of Alloys and Compounds, vol. 859, pp. 158219.
33. Zhou, H., Sun, Y., & Zhang, Z. (2016), Effects of Zinc Concentration on the Microstructure and Properties of Nanocrystalline Films, Journal of Materials Science, vol. 51, no. 14, pp. 6693-6703.
34. Hasan, M.M., Hasseeb, A.S.M.A., Saidur, R.& Masjuki H.H. (2008) Effect of annealing treatment on optical properties of anatase TiO2 thin films International Journal of Chemical and Bimolecular Engineering, Vol.1, pp.93-97.
35. Abdullah, M. T., Raoof, L. M., Hasan, M.H., Abd, A.N. & Mohammed, I.M., (2021)The Effect of Different Thickness on The Optical and Electrical Properties of TiO2 Thin Films journal of physics: conference sereis 1999,012128. DOI 10.1088/1742-6596/1999/1/012128
36. Marien, J., Wagner, T., Duscher, G., Koch, A. & Rühle, M.(2000) Ag, Pt, Pd, Nb Doping (110) TiO2 (Rutile): Growth, Structure, and Chemical Composition of the Interface, Surface Science, Vol. 446, P.219.
37. Mustafa, Y.& Abdullah, A. (2022) Effect of annealing temperature on the structural, optical and topographical properties of cadmium oxide (CdO) nanoparticles Samarra Journal of Pure and Applied Science, 4(3).
38. Hassan, M., Haseeb, A., Saidur, R. & Masjuki, H. (2008) Effects of Annealing Treatment on Optical Properties of Anatase TiO2 Thin Films World Academy of Science, Engineering and Technology, Vol. 40, PP. 221-225.
39. Rusul, A., Abbas, A. & Abbas, S. (2021) OPTICAL PROPERTIES OF ZnO FILMS PREPARED BY CBD TECHNIQUE Journal of Ovonic Research, 17(1), PP. 53-60.
40. Nibras, M., Afrah, R., Salih, Y. & Adil, A. (2023) Using Thermal Spraying by Flame to Calculate the Physical Parameters of a Nickel Based Samarra Journal of Pure and Applied Science, 5(1), PP. 160-169.

IRAQI Academic Scientific Journals
Samarra Journal of Pure and Applied Science
SJPAS
مجلة سامراء للعلوم البحتة والتطبيقية
www.sjpas.com
p ISSN: 2663-7405
e ISSN: 2789-6838

تأثير التشويب على الخصائص التركيبية، السطحية، التشكيلية والبصرية للاغشية الرقيقة لثاني اوكسيد التيتانيوم

هيام جاسب مجيد[1]، هبة سعد رشيد[1]، رسل عدنان حيدر الوردي[2]*
1-قسم الفيزياء كلية التربية، الجامعة المستنصرية، بغداد، العراق.
2- فرع العلوم المختبرية السريرية، كلية الصيدلة، الجامعة المستنصرية، بغداد، العراق.

معلومات البحث:
تأريخ الاستلام:2023/03/19
تأريخ القبــول: 2023/04/26
الكلمات المفتاحية:
ثاني اوكسيد التيتانيوم، التشويب بالزنك، تقنية التحلل الكيميائي الحراري، XRD، AFM.

معلومات المؤلف
الايميل:
dr.rusuladnan@uomustansiriyah.edu.iq

الخلاصة:
حضّرت أغشية رقيقة من أوكسيد التيتانيوم النقية والمشوّبة بالزنك بمعدلات (0، 2 و 4) عن طريق دمج أسيتات الكادميوم مع أسيتات الزنك في محلول من أسيتات التيتانيوم (0.2 مولاري) .أظهرت فحوصات XRD أن أغشية TiO_2 و (TiO_2: Zn) متعددة البلورات مع اتجاه (121). بالإضافة إلى ذلك، يرتفع تبلور الأغشية مع ارتفاع مستوى التطعيم بالزنك .مع تركيز التطعيم بالزنك، يكون حجم حبيبات الأغشية المترسبة حوالي (17.91-15.55) نانومتر، بينما تقل معامل الانفعال (٪) من 22.29 إلى 19.35 بالزنك .كان الحجم الحيبي في حدود (90.9) و (67.8) و (37.7) نانومتر لـ ($Ti O_2$, TiO_2: 2% Zn, TiO_2:4% Zn) وفقًا لذلك في صور AFM لتشكل سطح الفيلم .خشونة السطح وقيم جذر متوسط التربيع للأغشية المترسبة لـ ($Ti O_2$, TiO_2: 2% Zn, TiO_2:4% Zn) كانت (6.72، 3.34 و2.034) نانومتر و (8.80، 8.03 و4.24)، على التوالي. تم استخدام طيف الامتصاصية والنفاذية لدراسة الخصائص البصرية .الفحوصات أوضحت أن الأغشية لديها انتقال قوي عبر الطيف المرئي وأن النفاذية يتناقص مع زيادة التشويب بالزنك .بالإضافة إلى ذلك، تتغير حافة امتصاص للاغشية إلى أطوال موجية عالية، مما يدعم انخفاض قيم فجوة الطاقة .كما تم حساب واكتشاف الاختلاف مع زيادة تركيز الزنك في معامل الامتصاص، معامل الانكسار.